



Since January 2020 Elsevier has created a COVID-19 resource centre with free information in English and Mandarin on the novel coronavirus COVID-19. The COVID-19 resource centre is hosted on Elsevier Connect, the company's public news and information website.

Elsevier hereby grants permission to make all its COVID-19-related research that is available on the COVID-19 resource centre - including this research content - immediately available in PubMed Central and other publicly funded repositories, such as the WHO COVID database with rights for unrestricted research re-use and analyses in any form or by any means with acknowledgement of the original source. These permissions are granted for free by Elsevier for as long as the COVID-19 resource centre remains active.



New findings on impact of COVID lockdown over terrestrial ecosystems from LEO-GEO satellites

Nikhil Lele^{*}, Rahul Nigam, Bimal K. Bhattacharya

Agriculture and Land Eco-system Division, Biological and Planetary Sciences and Applications Group, Earth, Ocean, Atmosphere Planetary Sciences and Applications Area, Space Applications Centre (ISRO), Ahmedabad, 380015, Gujarat, India

ARTICLE INFO

Keywords:

Positive impacts
Terrestrial ecosystems
COVID
Lockdown
Space-based observations

ABSTRACT

The COVID 19 pandemic led to lockdown and restrictions on anthropogenic activities not only in India but all over the world. This provided an opportunity to study positive effects on environment and subsequent impact on terrestrial ecosystems such as urban, peri-urban, forest and agriculture. A variety of studies presented so far mainly include improved air quality index, water quality, reduced pollutants etc. The present study focused on few novel parameters from both polar and geostationary satellites that are not studied in context to India, and also attempts deriving/quantifying benefits rather than merely indicating qualitative improvements. Due to lack of anthropogenic activities during complete lockdown-1 (21 days from 25 March 2020) in India nighttime cooling of land surface temperature (LST) of the order of 2–6 K was observed. Amongst 10 major cities, Bhopal showed highest nighttime cooling. The cooling effect in LST was evident in 80% of industrial units distinctly indicating cooling trend. Vegetation fires were analyzed in 10 fire-prone states of India. Compared to past four-years average number of occurrences, only 45% fire occurrences occurred during lockdown, indicating strong effect of lockdown. The study also revealed that, there is increase in gross primary production in forest ecosystem to the tune of maximum 38%, during this period. Though delay in rabi crop harvest date by 1–2 weeks in majority of north Indian states was observed rise in rabi crop productivity of the order of maximum 34% was observed which is attributed to favorable environmental conditions for net carbon uptake. About 18% reduction in volumetric agricultural water demand was estimated in Indo-Gangetic region, parts of Gujarat and Rajasthan. Apart from controlling the spread of the disease, the lockdown restrictions were thus also able to show positive effects on the environment and ecosystem which might influence to rethink on strategies for sustainable development.

1. Introduction

Majority of the countries of the world were grabbed by severe acute respiratory syndrome coronavirus 2 (SARS-CoV-2) which was first reported from China. A novel Corona Virus Disease that was originated in December 2019, was named as COVID-19 by the World Health Organization (WHO). In the second week of January 2020, first case outside China was reported (www.covid19.who.int, 2020). The disease started rapidly spreading/getting detected in various countries. While in India, first case was detected on January 30, 2020; the rate of spread went on increasing and spread across all metropolitan cities and the state capitals. As a result, during third week of March, complete closure of places of mass gatherings (entertainment places, shopping malls, etc.) was

imposed. The WHO declared this as ‘pandemic’ on 11 March 2020, following which a large number of countries announced complete closure of activities (except essential and emergency services), which is referred as ‘lockdown’. China was the first country to go into two and half month’s lockdown starting from January 23. To control the rate of spread and number of casualties within India, lockdown was imposed by the Government of India 25 March 2020 onwards-initially for a period of 21 days and was later extended till 31st May in a phase-wise manner. Lockdown restrictions led to complete shutdown of all major industries, medium-scale enterprises (MSMEs), commercial hubs, construction activities, closure of almost all market commodities except the essential ones, vehicular traffic etc.

After the lockdown, significant changes in the environment

^{*} Corresponding author. ,

E-mail addresses: nikhillele@sac.isro.gov.in, nikhillele@sac.isro.gov.in (N. Lele), rahul.agmet@gmail.com (R. Nigam), bimal.vegetation@gmail.com (B.K. Bhattacharya).

<https://doi.org/10.1016/j.rsase.2021.100476>

Received 12 November 2020; Received in revised form 21 January 2021; Accepted 30 January 2021

Available online 10 February 2021

2352-9385/© 2021 Elsevier B.V. All rights reserved.

(primarily air quality and water quality) were noticed, studied and shared by large population in various parts of the world (Sharma et al., 2020; Siddiqui et al., 2020; Garg et al., 2020). There was no significant human activity on otherwise densely populated cities/roads. The fact triggered wild animals coming out of its territory. Images and videos of wild animals for example-elephants in Kerala, lions in Gujarat and Civet cats in Karnataka-roaming inside towns, were populated by social media users. Apart from this, a large number of scientific studies reported significant improvement in environment. Lal et al. (2020) showed a comparison of pollutants (such as NO₂, CO₂, aerosol optical depth), highlighting reduced industrial pollution at global scale vis-à-vis spread of the infection. Improvement in air quality was also observed at regional level in China and Europe (Zambrano-Monserrate et al., 2020), Brazil (Nakada and Urban, 2020), United states (Bermen and Ebisu, 2020) to name a few. All of the studies focused particularly on NO₂ and/or PM_{2.5} being primary indicators of pollution. In context to India, Sharma et al. (2020) reported reduced pollutant level and improvement in air quality index in 22 cities of India. Similar observations confirming improved air quality were reported by Lokhandwala and Gautam (2020), Mahato et al. (2020), Shehzad et al. (2020) Siddiqui et al. (2020), Singh and Chauhan (2020), Somani et al. (2020) and Srivastava et al. (2020) in major cities across India, many of them concentrating on Delhi, other metropolitan cities as well as densely populated Indo-Gangetic belt (Das et al. 2020, 2021). Significant reduction in forest fires was reported by Gupta et al. (2020) in parts of Western Himalayas, India. Not only in air quality, significant improvement was also reported in water quality in lake (Yunus et al., 2020), rivers (Garg et al., 2020) and ground water quality (Selvam et al., 2020) owing to minimal discharge of industrial wastes and slurry into rivers. These studies have merit of assessing environmental parameter(s) both qualitatively and/or quantitatively primarily for pollution aspects. But such lockdown might have left the other important imprints in the terrestrial ecosystem for rural and industrial sectors related to different economic activities which would enable decision makers to think on building new strategies for climate mitigation by taking short-term and long-term measures. Implications of such significantly reduced pollutants in environment over other ecosystems (such as urban, peri-urban, agriculture and forest etc.) though evident, were not quantifiably reported over India. Also, response of vegetation systems and feedback to environment as well as perceptible gain for betterment of human beings (for example improvement in carbon sequestration) are some of the gap areas from published studies. This paper focused on tracing reduced imprints of anthropogenic activities and atmospheric forcings in rural and industrial sectors using multi-temporal satellite data or products from both LEO (Low Earth Orbiting) and GEO (Geostationary Earth Orbiting) platforms. Four new aspects have been covered to assess and quantify such as (i) night-time surface cooling especially in cities and industrial sectors, (ii) vegetation fires, (iii) impact on crop harvest and productivity and (iv) impact on agricultural water demand due to the lockdown effect.

In tropical and sub-tropical climate such as in India and other Asian countries, night-time cooling is essential as it offers relief from heat wave, particularly during March to May and is very relevant in terms of electricity consumption, human comfort and even mortality. Night-time land surface temperature (LST) is, therefore, widely studied in urban environment (Holmes et al., 2013; Gao et al., 2005) to detect heat island and its variability. Throughout the day-time, urban surfaces absorb incident solar radiation. Particularly the dark surfaces (such as roads) absorb significantly more solar radiation and tend to warm faster. Materials commonly used in urban areas such as concrete and asphalt, have significantly different thermal bulk properties and surface radiative properties (such as albedo and emissivity) than the urban surroundings. Surfaces have differential emission characteristics for longwave infrared radiation (LWIR) in 8–14 μm , short-wave infrared radiation (SWIR) in 1.2–2.5 μm and middle infrared (MWIR) radiation in 3–5 μm wavelength regions of electromagnetic spectrum. During daytime in presence of sun,

the emission responses are a mix of LWIR, SWIR and MWIR, while during night time, only LWIR dominates the emission. In addition, thermal stability remains high during night-time due to lesser depth of nocturnal boundary layer and over near-neutral atmospheric stability conditions. This forms the basis of using night-time LST for quantifying heatwave and cold wave situation. The LST of urban and industrial landscape in peri-urban areas are influenced by presence of concrete/asphalt structures (buildings and roads), urban pollutants and anthropogenic aerosols in the atmosphere particularly due to burning of fossil fuels, and emissions from industries. Emission of pollutants is one of the most important aspects of human activities in urban and peri-urban industrial areas (McDonnell and MacGregor-Fors, 2016). The present study investigates the effect of reduced level of pollutants and emissions during lockdown phase on night-time LST.

In rural India, majority of the vegetation fires are anthropogenic in origin. These fires can be classified as crop fires, where fields are burnt post-harvest for easy manure during the next crop; and forest fires, which are unintentional, occur due to negligence and ignorance of forest dwellers as well as recreation activities majority of which are anthropogenic in origin (Satendra and Kaushik, 2014). Fires are typically seen to start at the end of January and rapid increase during the months of February to May. Vegetation fires are well-detected by the majority of the MWIR sensors using hot-spot detection technique and is provided as product to the user community (Joseph et al., 2009).

Crop growth cycle in an agricultural season is influenced primarily by weather variables such as temperature, humidity, bright sunshine hours (Mathison et al., 2018) as well as planting and harvesting dates determining length of growing season. The fluctuations in weather variables in critical crop growth stages during vegetative and reproductive phases can alter the occurrence and duration of phenological events. The lockdown period coincided with the maturity and harvesting periods of many *rabi* (post south-west monsoon corresponding to November to April) crops in northern India. In current study, we investigate the impact on *rabi* harvest in different north Indian states and crop productivity due to combined effects of restricted movement but with better environmental quality during COVID lockdown. Agricultural water demand is important aspect for water management and water savings (Shweta et al., 2018). We have also investigated impact of sudden change in weather and environmental conditions on agricultural water demand in different north Indian states through atmospheric evaporative demand in terms of reference evapotranspiration and crop coefficient.

2. Study area and datasets

2.1. Study area

The study area is Indian landmass which comprises of 329 ha with population of nearly 1380 million (www.worldometers.info, 2020) and is situated in the tropical region with the geographical extent spanning from 8.06°N to 37.10°N and 68.11°E to 97.41°E. India has 58% total geographic area as cropland, 22% area under forests and 6% area under urban (NRSC, 2014). India ranks second in global population, accounts for 17% of global population, with its 31% population staying in urban areas. Majority of the urban areas are associated with medium to large-scale industrial zones of various nature and are typically located in the fringe areas of the cities otherwise called peri-urban patches. Industrial and vehicular pollution are at very high levels in majority of the cities with average PM_{2.5} value for the country to be 58 $\mu\text{g m}^{-3}$, while ambient value in major cities including Delhi was found to be in the range of 130–170 $\mu\text{g m}^{-3}$.

India is the hub of industries including pharmaceuticals, textiles, automobiles, consumer products and warehousing. Certain parts of the country such as regions surrounding Delhi (states of Haryana, towns such as Gurgaon, Noida), Maharashtra (cities like Pune, Nasik, Aurangabad), West Bengal (Asansol, Durgapur, Haldia), Gujarat (Sanand,

Dahej, Kalol, Mundra port), Tamilnadu (Sriperumbadur, Oragadam), are few such large industrial zones in India, with Tamilnadu having largest number of factories in India (Invest India, 2020). Apart from industries, large-scale information technology parks exist in cities like Noida, Hyderabad, Pune, Bengaluru and Chennai. The land use land cover map overlaid with distribution of large industrial areas more than 3 sq. km is

shown in Fig. 1.

Other than industries, agriculture is primary source of livelihoods for over 70% of population in India and rural India contributes approximately 17% in the country's Gross Domestic Product (GDP). Rainfed and irrigated systems are commonly practiced in croplands of India, with rainfed system constituting 51% of country's agriculture area (MoAFW,

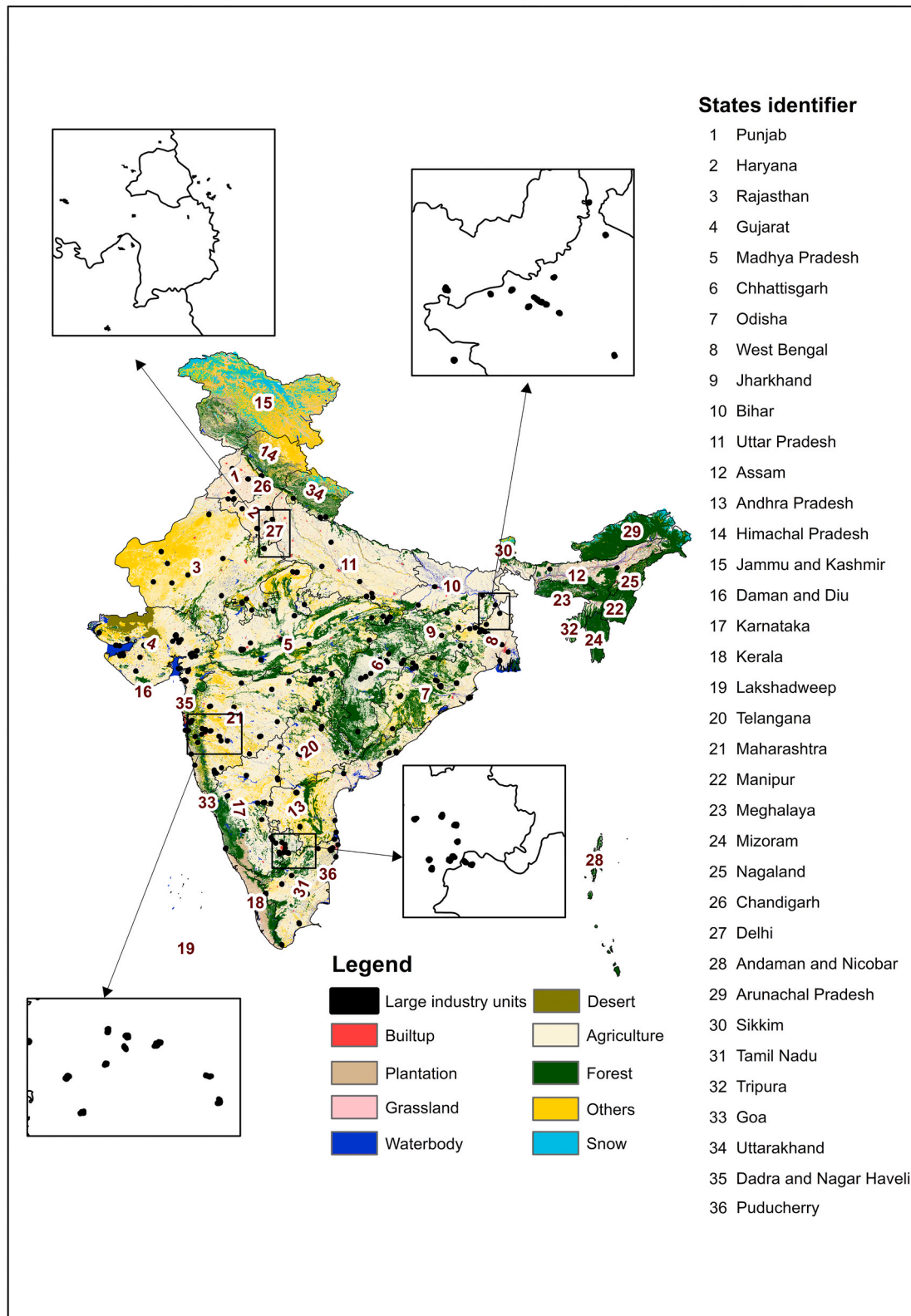


Fig. 1. Land use land cover map of India overlaid with locations of large-scale industrial units having areas more than 3 sq km across different states.

2017).

2.2. Datasets

2.2.1. Satellite datasets

The study utilizes both sun-synchronous polar or low-earth orbiting (LEO) and geostationary (GEO) satellite observations from Indian and global missions. Among these, the LEO satellites are MODIS (Moderate Resolution Imaging Spectroradiometer), Suomi-NPP (Suomi-NPP (Suomi NPOESS Preparatory Project), SMAP (Soil Moisture Active Passive) and GEO satellite is INSAT (Indian National Satellite) 3D. The satellite data and the bio-geophysical products used from these LEO-GEO satellites in the present study, are given in Table 1.

Among the LEO missions, MODIS (Moderate Resolution Imaging Spectroradiometer) instrument is operating over AQUA and TERRA platforms and has capability to sense the data over 36 spectral channels spanning across visible to longwave infrared bands (from 0.4 μm to 14.4 μm) at varying spatial resolutions of 250 m, 500 m and 1000 m. This provides capabilities to map not only the land cover features (such as vegetation, water, open areas) but also atmospheric constituents like water, ozone and also land surface temperatures (LST). MODIS has ability to observe majority of the earth surface at daily interval and therefore is one of the most widely used instruments for a wide number of applications. Various products and datasets are provided to global user community via multiple data archival systems (e.g. www.earthexplorer.gov). A large number of standard products for land, ocean, air and cryosphere are routinely generated using MODIS data and are distributed to global scientific community.

MODIS land surface temperature (LST) is retrieved at 1 km spatial resolution based on day-night algorithm. In the present study, night-time LST of MODIS AQUA at 130 AM retrieved from 7 thermal infrared bands (Wan, 1999) were used. MODIS vegetation indices and canopy-related products are produced as 8-day composites. Normalized Difference Vegetation Index (NDVI) product is derived from atmospherically corrected bi-directional surface reflectance. The product provides consistent spatial and temporal vegetation properties and are commonly used in ecosystem and climate change studies (Huete et al., 1999). The MODIS TERRA eight-day product (MOD17A2H) on gross primary productivity (GPP) at 500 m spatial resolution was acquired for the period of November–May during successive *rabi* seasons (2018–2020). The data for the whole India were acquired from the EOS data gateway. The product is based on the radiation-use efficiency concept (Monteith, 1977). The inputs for GPP product are satellite-derived FAPAR (fraction absorbed photosynthetically active radiation), surface insolation from global meteorology, modelled ambient temperature and vapor pressure deficit from land surface temperature and radiation conversion efficiency factor (Running et al., 2000).

Table 1
Details of data and bio-geophysical products from LEO-GEO satellites.

Satellites	Sensors	Product name	Product code/version	Period	Spatial resolution (m)	Temporal resolution	Source
MODIS (LEO)	AQUA	LST	MYD11A1 version 6	1 January to 15 April	1 km	Night-time	www.earthexplorer.usgs.gov
	TERRA	NDVI	MOD13A2 version 6	2019 and 2020	500 m	(130 AM)	
	TERRA	GPP	MOD17A2version 6	22 March to 6 April	1 km	Daily	
SUOMI-NPP (LEO)	VIIRS	Vegetation fire	VNP 14 version 6	2019 and 2020	375 m	8-day composite	www.firms.modaps.eosdis.nasa.gov
				2016 to 2020			
SMAP (LEO)	L-band radiometer	NASA-USDA-SMAP Global soil moisture	NASA_USDA_HSL_soil_moisture	March and April	27 km	Daily	Google earth engine
INSAT 3D (GEO)	Imager	Reference Evapotranspiration (ET ₀)	3D_IMG_L3C_PET_DLY. Version 1.	26 March to 10 April	4 km	Daily	www.mosdac.gov.in
				2018, 2019 and 2020			

The NASA Suomi-NPP VIIRS (Suomi NPOESS Preparatory Project-Visible Infrared Imaging Radiometer Suite) sensor aboard NOAA satellite has been providing vegetation fire product based on combination of visible and thermal infrared bands. Based on I1 to I5 high resolution spectral channels (0.640 μm , 0.865 μm , 1.610 μm , 3.740 μm and 11.45 μm), complemented by M13 spectral channel (4.05 μm) from middle infrared region, VIIRS provides daily product of vegetation fires. In comparison to MODIS fire, VIIRS fire product is available at spatial resolution of 375 m and has better response for detecting vegetation fires of smaller area (Giglio et al., 2016). Under pristine observation conditions (though rare in reality) it can detect fires up to 50 sq m in size (www.earthdata.nasa.gov).

A L-band radiometer aboard SMAP (Soil Moisture Active Passive) satellite is designed to detect presence of water in top layer (within \sim 0.1 m depth) of the soil. The surface soil moisture was used to analyze soil moisture variability in the year 2020 to understand any events related to subsequent changes in soil moisture.

INSAT 3D (Indian National Satellite) is the geostationary satellite over India region which provides frequent observations at 4 km spatial resolution over India and surrounding region. INSAT has 6 spectral channels (1 in visible region, 1 in shortwave infra-red region and 2 each from middle infra-red and longwave infra-red and data are distributed to research community through MOSDAC (Meteorology and Oceanographic Satellite Data Archival Centre: www.mosdac.gov.in) (IMD, 2014). Reference evapotranspiration (reference ET or ET₀) product is generated based on a fusion approach using daily insolation product from INSAT 3D Imager and gridded short-range weather forecast of non-radiative variables from NWP model within FAO56 model framework employing algorithm used by Vyas et al. (2016). Reference ET describes evaporative demand of the atmosphere for a given climatic region and basic input to compute crop water demand.

2.2.2. Ancillary datasets

Ancillary datasets comprise of shapefile of industrial layer which was acquired from OpenStreetMap (OpenStreetMap, 2020). Polygon layer of industries was used and polygons with area ≥ 3 sq km (indicating large industrial units) were used for analyzing night-time LST changes (Δ LST) and to extract mean values for each polygon of layer. National forest cover of India (year 2015) procured from Forest Survey of India (FSI, 2015) was used to analyze fires belonging to forest areas. Further, pan evaporation data during April (1–30) and May (1–20) for year 2018, 2019 and 2020 were acquired from limited number of agro-meteorological observatories viz. (i) Punjab Agricultural University, Ludhiana (30.90°N and 75.80°E) (ii) Rajendra Agricultural University, Samastipur, Bihar (25.85°N and 85.78°E), (iii) Rajasthan Agricultural Research Institute, Jaipur (26.84°N and 75.79°E) and (iv) Main Rice Research Station, Nawagam, Gujarat (22.79°N and 72.57°E) in this study.

3. Methodology

Satellite data and bio-geophysical product variables from different satellites and available sources (hereafter referred as ‘inputs’) were processed using various ‘functions’ that include data processing algorithms and value additions such as flexible time-compositing, maximum value compositing, trend analysis and anomaly detection. The ‘end outputs’ refer to spatio-temporal hot-spots or indicating drastic changes in specific variables. The flow chart of overall methodology is given in Fig. 2.

The study adheres to existing operational satellite data and products following the lockdown limitations for ground data collections and impacts on various parameters are primarily studied by detecting anomaly in various products and analyzing spatio-temporal trends with respect to past years. The methodology has been elucidated here:

3.1. Detection of night-time surface cooling

MODIS–AQUA night-time (130AM) LST product was analyzed to find the difference for similar time periods between 2019 and 2020 during January, February, March and up to first fortnight of April. Difference of LST (denoted as ΔLST_{night} , hereafter) was calculated as:

$$\Delta LST_{night} = LST_{night(2019)} - LST_{night(2020)}$$

Positive ΔLST_{night} indicates the cooling of land surfaces in the night-time. The ΔLST_{night} was computed for 2 temporal steps: (i) Prior to lockdown i.e. during 1 March to 24 March and (ii) Post-lockdown i.e. during 25 March to 10 April. In addition, monthly night-time LST were also computed for January, February months for both 2019 and 2020. Maximum value compositing was made for the generation of monthly, pre-lockdown and post-lockdown LST. Anomaly detection of ΔLST_{night} was analyzed over 6 prominent cities of India (viz. Delhi, Lucknow, Allahabad, Bhopal, Pune and Hyderabad). Other metro cities of India (such as Mumbai, Chennai and Kolkata) experience strong maritime weather and also experience frequent rainfall being situated in coastal areas. Changes in LST can be better studied at places that have continental climate and do not receive frequent rainfall in the summer season. In addition to such urban areas, ΔLST_{night} was analyzed over prominent industrial zones of the country-that are typically located in peri-urban regions. In view of coarser spatial resolution (~1 km) of MODIS LST data, smaller industrial units were not considered for the study, and moderate and large units with polygon areas ≥ 3 sq km were analyzed. Magnitude of ΔLST_{night} anomaly over city and industrial

locations were studied.

3.2. Counting anomaly in vegetation fires

The fire product of Suomi NPP-VIIRS were analyzed for detecting number and occurrences of vegetation fires with ‘high confidence’ for lockdown period in the year 2020. Vegetation fires corresponding to the similar periods for past 4 years (2016 to 2019) were also averaged and compared with number of fires occurred during year 2020. Further, in order to understand the effect on activities and movements of native populations in remote areas (away from cities and towns), number of fire locations lying within and outside 3 km buffer distance of road were analyzed. Occurrences of fire in past years and anomaly in the 2020 lockdown period were computed in nine fire-prone states of India viz. Jharkhand, Karnataka, Kerala, Madhya Pradesh, Maharashtra, Odisha, Rajasthan, Tamilnadu and Uttaranchal, respectively.

3.3. Estimating agricultural water demand

Daily reference evapotranspiration (ET_0) product of INSAT 3D from March 15 to May 20, for three years (2018, 2019 and 2020) were acquired from MOSDAC (www.mosdac.gov.in) and used in the present study. The daily MODIS NDVI data at 500 m were also used in this study for the aforementioned period. The daily MODIS NDVI data was sampled at parent resolution of ET_0 (0.04°) product (Nigam and Bhattacharya, 2015; Vyas et al., 2016). In this study, agricultural mask was used (NRSC, 2014) and re-sampled at target spatial resolution (4 km) of ET_0 through linear aggregation. The district weighted crop specific area has been computed from statistics data published by Department of Agricultural Co-operation for *rabi* and *kharif* seasons. Crop coefficient (K_c) is taken for particular crop type from Allen et al. (1998). The area weighted generalized agricultural K_c was computed. The MODIS NDVI was used to generate vegetation fraction (F_c) over agricultural area. The sigmoidal model between F_c and K_c (Choudhury and Bhattacharya, 2018) for *rabi* (November to April) was used in the present study to generate crop evapotranspiration (ET_c) under non-stressed conditions (Allen et al., 1998). The summation of ET_c for 1–30 April and 1–20 May was made to generate agricultural water demand (AWD) for agricultural crops.

3.4. Characterizing anomaly in harvest date and productivity of rabi crops

The daily MODIS TERRA data were used to estimate harvest date of

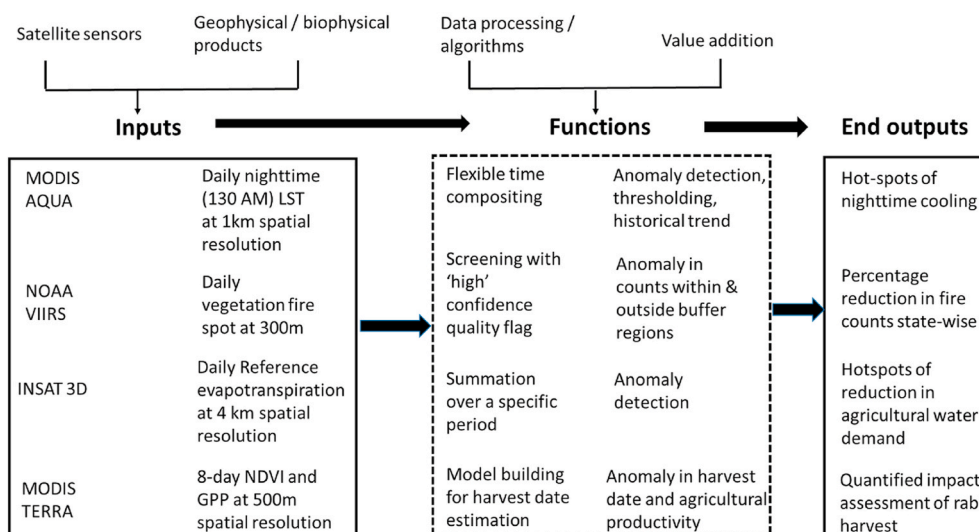


Fig. 2. Brief methodology for parameters analyzed towards assessing impact of lockdown.

rabi crop for agriculturally dominant states of India. From daily NDVI data, 5-day composite was prepared for March 10 to May 15, to generate time profile curve of NDVI for mean (2016–2019) and year 2020. To prepare composite of 5 days, maximum NDVI value was taken during those respective 5-days. This minimizes the cloud and atmospheric perturbations in NDVI data set. An additional lag period of 2 days is required for spectrally detecting the harvest from coarse resolution satellite. Thus, a compositing period of 5-days was optimized to detect harvest date crossing pre-determined NDVI threshold. In this study, standard agricultural mask from land use land cover (LULC) map (NRSC, 2014) was used which was resampled at parent spatial resolution of MODIS (1 km × 1 km) through linear aggregation and was applied over each 5-day NDVI composite to retain over agricultural pixels only. Two stacks were prepared from March 10 to May 15, from 5-days' NDVI composite and NDVI profiles were generated for each agricultural pixel for year 2020 and mean from year 2016–2019. Similarly, Vyas et al. (2013) and Sakamoto et al. (2005) also used NDVI profile to detect crop sowing date using INSAT3A CCD and MODIS data, respectively. On the basis of NDVI profile, following mathematical expression was applied to model the behavior of NDVI profile for each pixel and extract harvest date.

$$\text{IF } (NDVI_i < C_1 \ \& \ NDVI_{i-1} - NDVI_i > C_2) \ \& \ (NDVI_{i+1} - NDVI_{i+2} > C_3) \ \text{THEN Harvest date (HD)} = i - 2$$

Where, C_1 , C_2 & C_3 are thresholds (>0) and $NDVI_{i-1}$, $NDVI_i$, $NDVI_{i+1}$ and $NDVI_{i+2}$ are $i - 1^{st}$, i^{th} , $i + 1^{th}$ and $i + 2^{nd}$ 5-day temporal NDVI composites, respectively.

The model was applied to NDVI profile in such a way that it was able to pick the date of inflection point where NDVI dropped due to harvest of *rabi* crop and after that NDVI profile started decreasing with a persistent negative gradient due to harvest of *rabi* crop. The change in behaviour of NDVI profile was detected on the basis of change in NDVI minimum threshold value of 0.3 with persistent negative slope and harvest date was estimated for *rabi* crop in agriculturally dominant states by deducting 2 days from the day of inflection point. The NDVI profile of

different agro-climatic zones under the study region is shown in Fig. 3. In-situ *rabi* harvest date observations over limited locations were collected in parts of Punjab and Rajasthan states for validation even in restricted movement during lockdown.

4. Results

This section highlights the reduced anthropogenic impact due to lockdown-1 on key environmental factors of urban and rural ecosystem. Night-time surface cooling was assessed over dominant industrial zones in urban proximity (peri-urban region) while vegetation fires, anomaly in harvesting date and agricultural productivity and crop water demand during *rabi*-summer cropping season were assessed in selected agroecosystems.

4.1. Night-time cooling pattern of urban and peri-urban industrial regions

The deviation in night-time MODIS LST (ΔLST_{night}) in 2020 from 2019 before and after lockdown-1 periods revealed that a major part of India indicated cooling of land surfaces. Majority of the eastern and southern part of the country showed 0–2 K cooling during this period, while drastic large cooling was noticed in northern and central-western parts of the country such as Delhi, Gujarat, Madhya Pradesh, Maharashtra, Rajasthan, Uttar Pradesh and Assam states (Fig. 4). Part of north Gujarat showed highest cooling ($\Delta LST_{night} = 6-8$ K). During pre-lockdown period (March 1 to March 24, 2020), the results indicated nominal cooling ($\Delta LST_{night} = 0-2$ K) only over part of southern India, Uttarakhand, southern Gujarat, part of West Bengal and negative cooling in the rest part of the country. It may be noted that nominal cooling was associated with those regions where cloud persistence and occurrence of rainfall are more during this period than rest of the country. This could have led to nominal cooling in those few patches majority of which, however, witnessed sudden and larger shift towards more cooling coinciding with lockdown period. A large part of northern India was in the grip of cooling of 2–4 K during lockdown.

Among the six cities having continental climate, maximum ΔLST_{night}

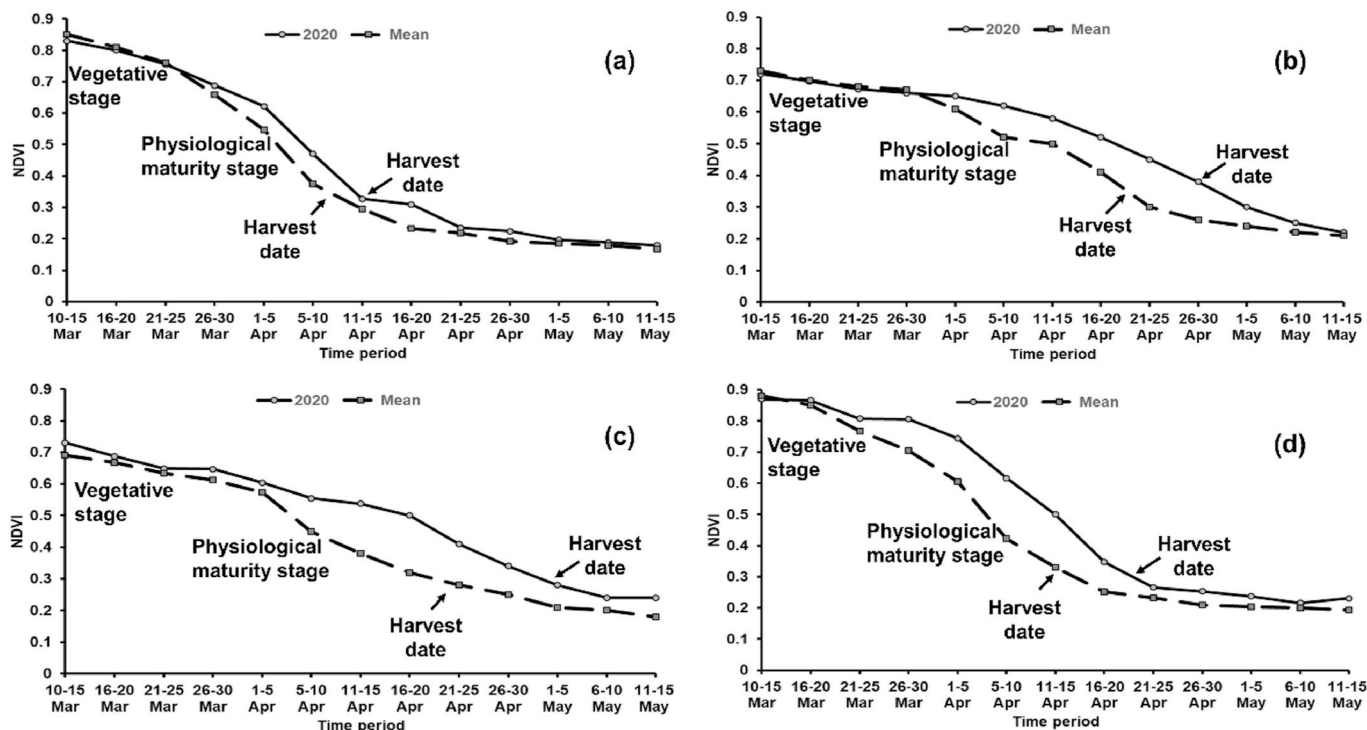


Fig. 3. Example of temporal NDVI profile for mean (2016–19) and 2020 (a) Trans-gangetic plain region; (b) Gujrat plain and hill region; (c) Middle gangetic plain region and (d) Lower gangetic plain region.

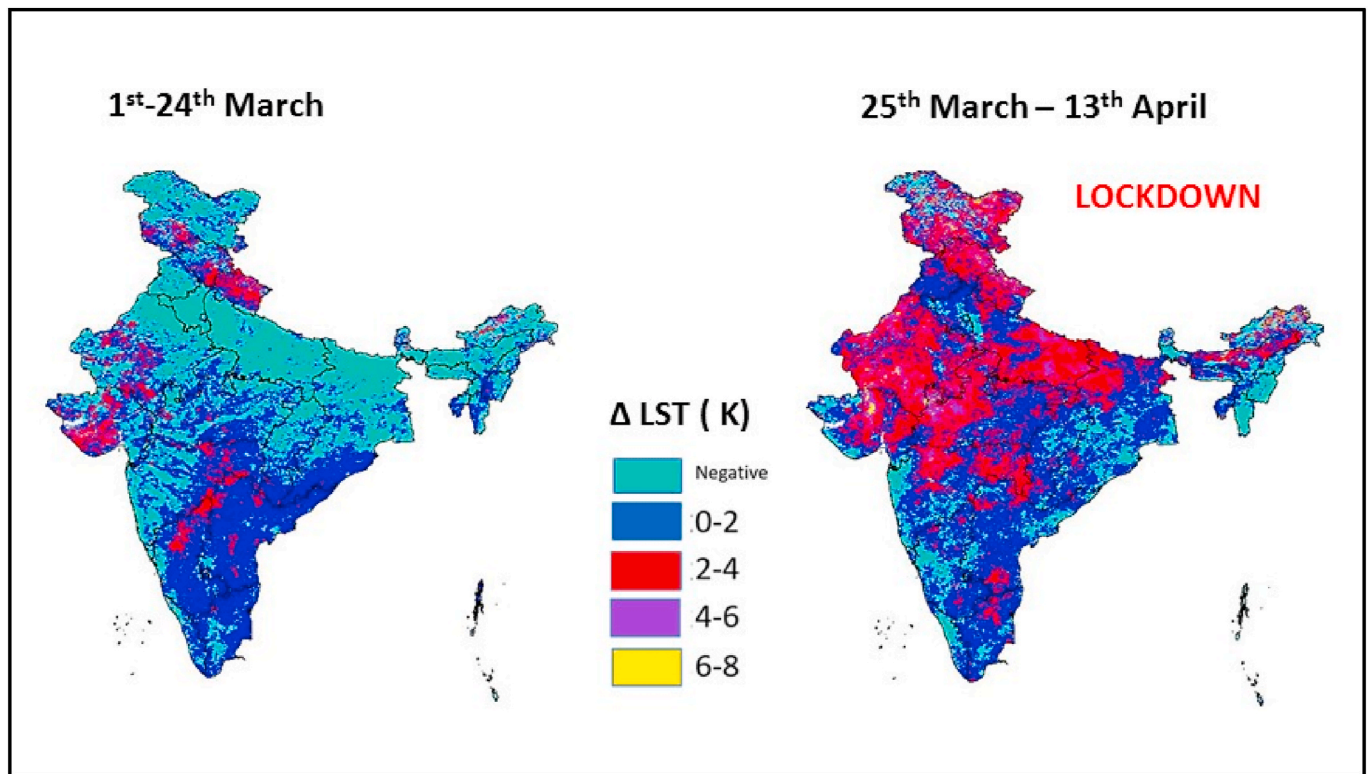


Fig. 4. Night time LST deviation from 2019 with more cooling in year 2020 during pre-lockdown and lockdown-1.

of the order of 2.3 K was noticed in Bhopal (23.25° N and 77.41° E) while least cooling (0.4 K) was observed in Pune (18.52° N and 73.85° E). Other cities also showed night-time cooling close to 1 K (viz. Bengaluru (12.97° N and 77.59° E): 0.7 K, Lucknow (26.84° N and 80.94° E): 1 K, Delhi (28.70° N and 77.10° E) and Hyderabad (17.38° N and 78.48° E): 1.1 K, and Allahabad (25.43° N and 81.84° E): 1.6 K). Analysis of surface soil moisture data from SMAP over major industrial clusters showed average decrease of 2.6% in monthly mean soil moisture from March to April indicating no influence of rainfall on reduction in LST. Metropolitan cities having maritime climate (such as Mumbai, Chennai and Kolkata) showed responses because of cloud and intermittent rainfall effect, therefore, not considered appropriate for present LST analysis. An

increase in mean monthly soil moisture from 18 – 50% during month of March and April was noticed in these cities, indicating the influence of intermittent rains, which would eventually lead to cooling of LST.

The ΔLST_{night} over large industrial units in the country showed an overall trend of night-time cooling in majority of the cases. Amongst 315 large-sized industrial units, 255 (80%) clearly indicated cooling effect (Fig. 5). Industries showing positive trend in cooling of LST indicated mean cooling of 1.4 K but varying in the range of 0.2–5 K.

4.2. Vegetation fires and primary productivity

The data on vegetation fire counts were analyzed for 24 March 2020

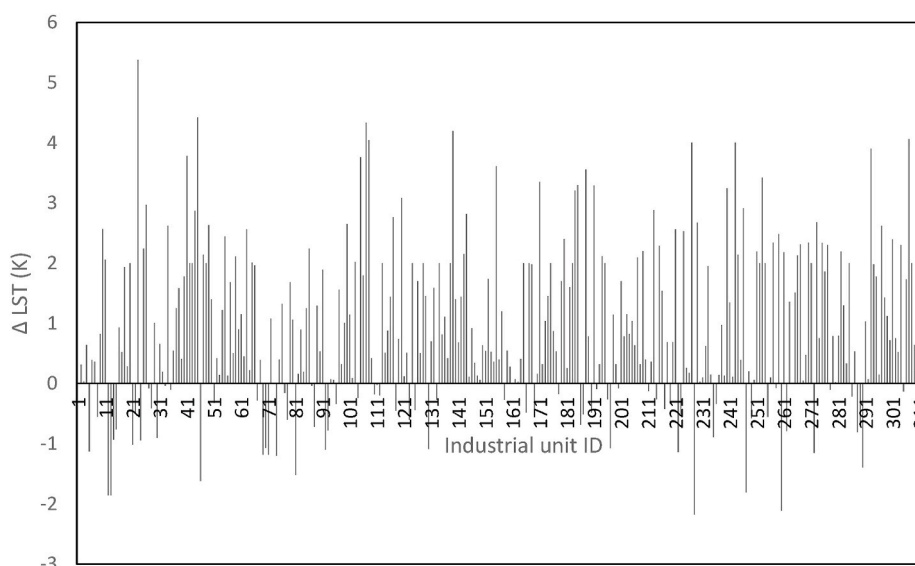


Fig. 5. Nighttime cooling (ΔLST_{night}) observed over large industrial units due to lockdown.

to 14 April 2020. In order to have the scenario of normal fire pattern during this period, data from year 2016–2019 for the same period was used. This particular time duration (end of the month of March and beginning of April) also coincides with burning due to shifting cultivation practices, which are dominantly found in north-eastern states of India and were not considered during the study (Alam, 2016). We have focused the present study on nine fire-prone states such as Jharkhand, Karnataka, Kerala, Madhya Pradesh, Maharashtra, Odisha, Rajasthan, Tamilnadu and Uttarakhand.

During 2016–19, average number of fire counts with ‘high’ confidence flag were considered for accounting for each state and were compared with 2020 data of the same periods. The states such as Madhya Pradesh, Maharashtra and Odisha showed highest fire counts in the past four-years’ average. Each of these states reported, respectively 57%, 75% and 65% lesser fire events during 2020 lockdown-1. Amongst other states, Jharkhand, Rajasthan and Uttarakhand reported reduction of fires (58%, 5% and 75%, respectively). Karnataka and Tamilnadu indicated rise in fire counts with majority of the fires in cropland areas (that particularly occur post-harvest) and very limited fires were observed in forest areas. During the span of 22 days about 1092 fire events were reported from these 10 states, which was 45% less as compared to four-years’ average (2376) of fire counts.

Further, number of fires were analyzed with respect to zone of influence to compare number of events near the towns/settlements and away from settlements. Fire events lying outside the 3-km buffer region around settlement and roads were referred as events from remote areas. It was found that in Kerala and Uttarakhand, all the fire events during this period occurred in remote areas. None of the fire events was observed inside the 3 km buffer thus strongly indicating effect of lockdown on human activities. Similarly, in Odisha and Jharkhand states, respectively 70% and 77%, of the total events in this duration occurred in remote areas. States such as Karnataka, Maharashtra, Rajasthan and Tamilnadu reported 56%, 44%, 44% and 42% events in remote areas, respectively. A further analysis in these 4 states (Karnataka, Maharashtra, Rajasthan and Tamilnadu) by overlaying fire events on land use land cover map indicated that majority of fires occurred in non-forest areas (or farm fires), indicating possible burning of crops residues after harvest. State-wise details are provided in Table 2, values with >70% are indicated in bold.

MODIS-GPP product for 2019 and 2020 was studied in order to analyze impact of reduced fires on primary productivity, particularly in forest ecosystem. Non-forest areas were masked from GPP product and productivity amongst only forest pixels were considered. In addition to forests fires, productivity indicates overall effect of other factors as well, that includes forest logging and lopping, which are other anthropogenic activities, though beyond the scope of the present study. Comparison of Gross Primary Productivity (GPP) product for 2019 and 2020 indicates higher rates of forest productivity in the year 2020. Maximum value composite of 8-day MODIS GPP Product showed 18.6 T g C/8-day (Terra gram Carbon) in 2019 while 25.1 T g C/8-day was found in 2020. This clearly suggests that due to better environmental conditions and much

reduced anthropogenic pressures (including fire, lopping, logging etc) a total of 6.5 T g C/8-day of gross primary production was additionally fixed during this particular period. Ten selected states accounted for 7.8 G g C/8-day during this period in 2019, while it accounted for 10.8 G g C/8-day, indicating 38% increase in gross primary production. These estimates thus suggest that there is an improvement in carbon fixation potential by primary producers and emission saving during lockdown period.

4.3. Impact on rabi harvest and agricultural productivity

The model for harvest date detection was applied to mean (2016–19) and 2020 NDVI temporal profiles to diagnose delay or early harvest for agricultural patches at 1 km spatial resolution primarily over selected 11 states of northern India. The *rabi* crop sowing is generally done at different time periods in those states of northern India (Fig. 6) due to differences in crop types, management practices and agro-climatic characteristics. These led to a large variation in harvest dates. The developed model was able to pick up the spatial pattern of harvest date in all the eleven states. General variation of harvest date as reported in various literatures is between first week of March to second week of May (<https://nfsm.gov.in>).

The comparison of estimated *rabi* harvest date for two states was made with observed date for year 2020. At 18 locations, ground observed data distributed over north and north-western states of Punjab and Rajasthan, respectively was compared with satellite estimated harvest date for *rabi* crops. The estimated harvest date for year 2020 showed RMSE of 4.2 (n = 18) days with R² of 0.88 with observed dates as shown in Fig. 7.

Spatial patterns of mean and 2020 *rabi* harvest estimated from satellite observations are shown in Fig. 6 (a) and 6 (b) alongwith histogram in Fig. 6 (c). The difference in *rabi* harvest date between mean and 2020 is shown in Fig. 8. The mean harvest date in Punjab and Haryana states was found to be within 1–20 April. But, in 2020, it was extended by 5–20 days. In this region, rice-wheat, cotton-mustard and cotton-wheat crop rotations are dominant (Anonymous, 2019; Sharma and Singh, 2014; Lata, 2014; Pinki et al., 2013). These different cropping patterns have different length of growing seasons. The mustard dominated regions of north-west part of Haryana and adjacent region of Punjab state showed difference of 5–15 days while wheat growing region showed a difference up to 20 days (Fig. 8).

The north-west and western parts of India covering Rajasthan and Gujarat states showed variation in estimated harvest dates from 25 March to 15 April. In this part of India, Pearl millet-cumin/isabgol, pulses-wheat and soybean/groundnut-wheat, cotton-wheat/fodder are dominant crop rotations (Jangid et al., 2018; Meena et al., 2017). This covers both irrigated as well as rainfed agricultural regions (Jaglan, and Qureshi, 1996). The northern part having canal command area showed delay in *rabi* harvest by 5–10 days in the year 2020 as compared to mean. Different time of maturity of *rabi* crop along with irrigation facility was the reason for different dates of sowing of *rabi* in many parts of this region. In central region, 15–20 days delay was observed in harvest date in 2020. Few crop patches across Rajasthan and Gujarat states, dominated by cumin and isabgol crop, showed early harvest by 5–10 days in the year 2020.

The states of Uttar Pradesh and Bihar showed wide range (25 March to 25 April) of mean harvest dates. This could be due to diverse crop rotation and crop type in different agro-climatic zones. The majority of agricultural patches, showed delay of 5–20 days in 2020 as compared to mean. Very few scattered patches in the middle of this region showed early harvest of 5 days. In Son command region of south-west of Bihar state, *rabi* crop harvesting is generally done in the first fortnight of April. In the year 2020, this region showed 10–20 days delay in harvest. The histogram in Fig. 6 (c) clearly showed the delay of harvest date in 2020 as compared to mean.

In Madhya Pradesh and Chhattisgarh states, the estimated *rabi* crop

Table 2
State-wise number of vegetation fires.

States	Average of 2016–2019	2020	% deviation from mean fire counts	% events away from towns
Jharkhand	43	18	–58	77.8
Karnataka	51	94	83	56.4
Kerala	22	5	–78	100
Madhya Pradesh	1321	569	–57	58.0
Maharashtra	439	111	–75	44.1
Odisha	320	111	–65	70.3
Rajasthan	88	83	–5	44.6
Tamil Nadu	81	98	22	41.8
Uttarakhand	12	3	–75	100

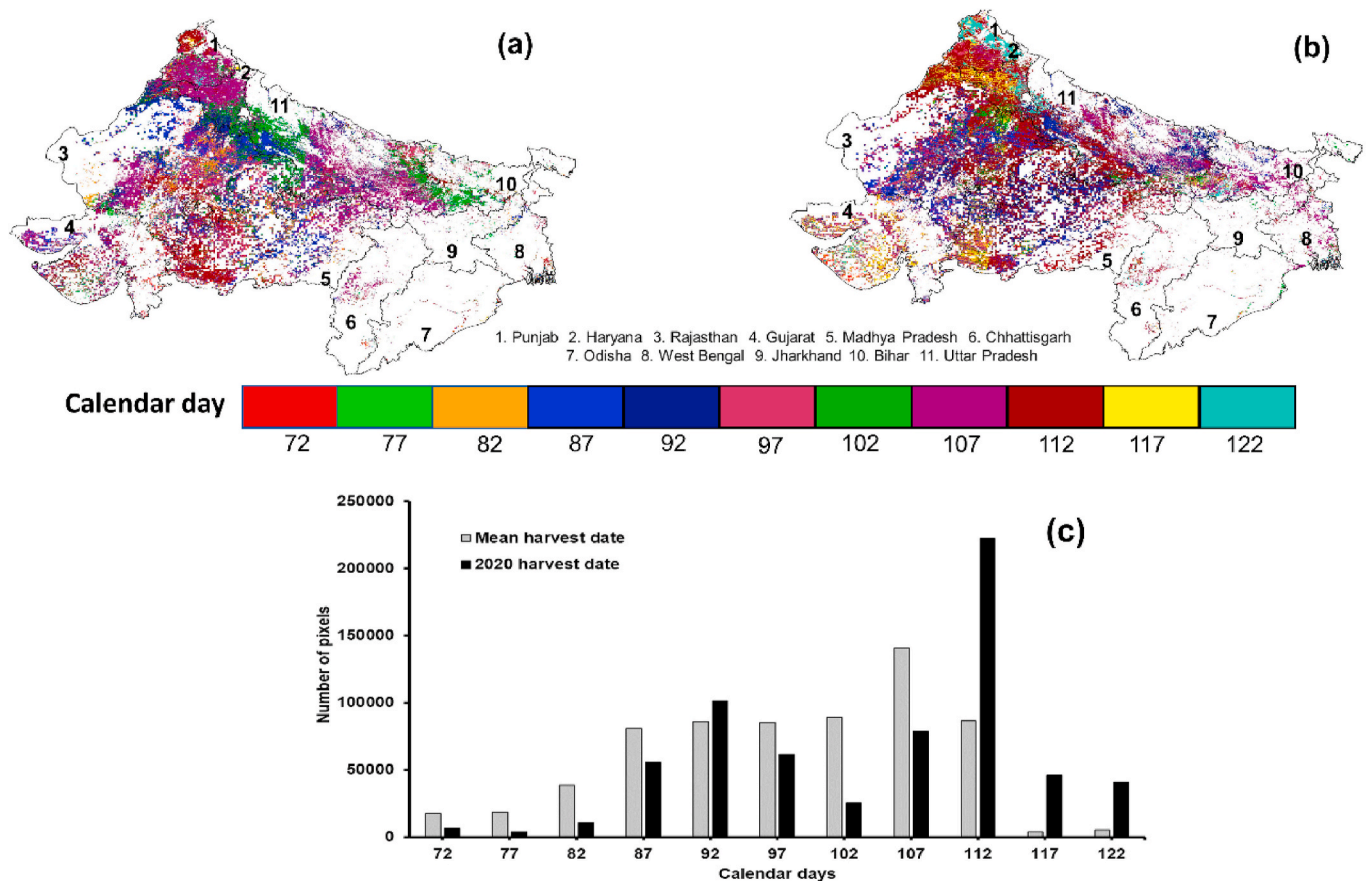


Fig. 6. Spatial distribution of (a) mean (2016–2019), (b) 2020 harvest date of *rabi* crops, (c) histogram of harvest dates.

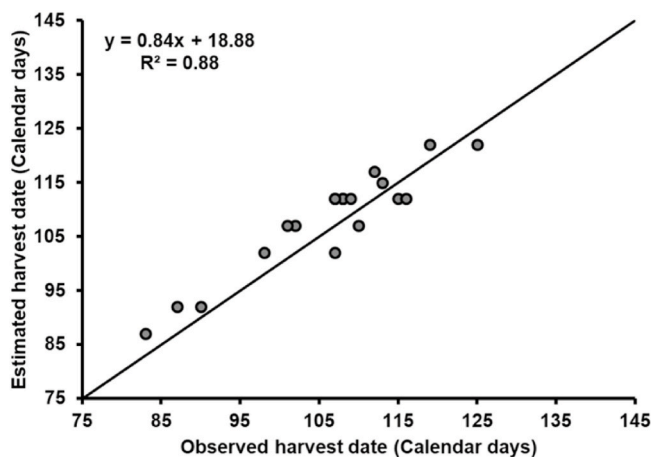


Fig. 7. Validation of satellite-based estimates of harvest date during 2020 over limited number of locations.

harvest date showed maximum diversity due to different crop types, sowing patterns and both irrigated and rainfed *rabi* crops. In the year 2020, maximum agricultural patches showed 10–20 days delay as compared to past years, except few fragmented patches of north-eastern part that showed early harvest in 2020. In eastern part of India covering West Bengal, Odisha and Jharkhand states only, small pockets showed delay in harvest dates by 5–15 days as shown in Fig. 8.

4.4. Impact on agriculture water demand (AWD)

An assessment of AWD during lockdown periods was made over

eleven (11) agriculturally enrich states of India. The mean AWD over agricultural patches was estimated from 2018 and 2019 for the periods 1–30 April and 1–20 May. The difference of AWD (in mm depth of water) between mean and year 2020 was computed. The percentage change in AWD for 2020, compared to mean is shown in Fig. 9. During April, in the northern states of Punjab and Haryana known as food bowl of India, the AWD was found to decrease in the range of 10–50 mm, particularly in the southern part of those states while large agricultural patches showed reduction of 40–80 mm in central and northern parts of those states. Maximum reduction in AWD of the order 140 mm was also noticed in few agricultural areas. In May, few scattered patches at foot hills of Himachal Pradesh showed low AWD in 2020 for short duration summer crops and long duration or perennial crop such as sugarcane, fruit crops. Few scattered patches in central portion of both the states having short duration summer vegetable crops showed decrease in AWD. The reductions in volumetric AWD in April and May 2020 were 8.6%, 11.1%, respectively in Punjab and 11.8%, 12.5%, respectively in Haryana (Fig. 10). The Uttar Pradesh state showed decrease of 4.4 and 8.5%, respectively with more impact in May than April AWD.

Substantial reductions in AWD were also noticed in north-west India (e.g. Rajasthan state) and central India (e.g. Madhya Pradesh state). The agricultural patches of Rajasthan, adjacent to Gujarat state growing summer vegetables and fodder crops, showed decrease in AWD in the range of 40–140 mm for both in April and May for year 2020 with overall reductions in volumetric AWD of 14.5% and 14%, respectively for those two periods. The reductions were 10.9%, 11.5% in Gujarat state and 13.9%–14.9% reduction in Madhya Pradesh state. In eastern India, reductions in volumetric AWD were also noticed in Bihar (10.7–13.2%), Jharkhand (12.3–15.1%), Chhattisgarh (13.2%) and Odisha (15.2%) states in the month of April which generally coincide with maturity of *rabi* crops. The crops such as rice and jute were at

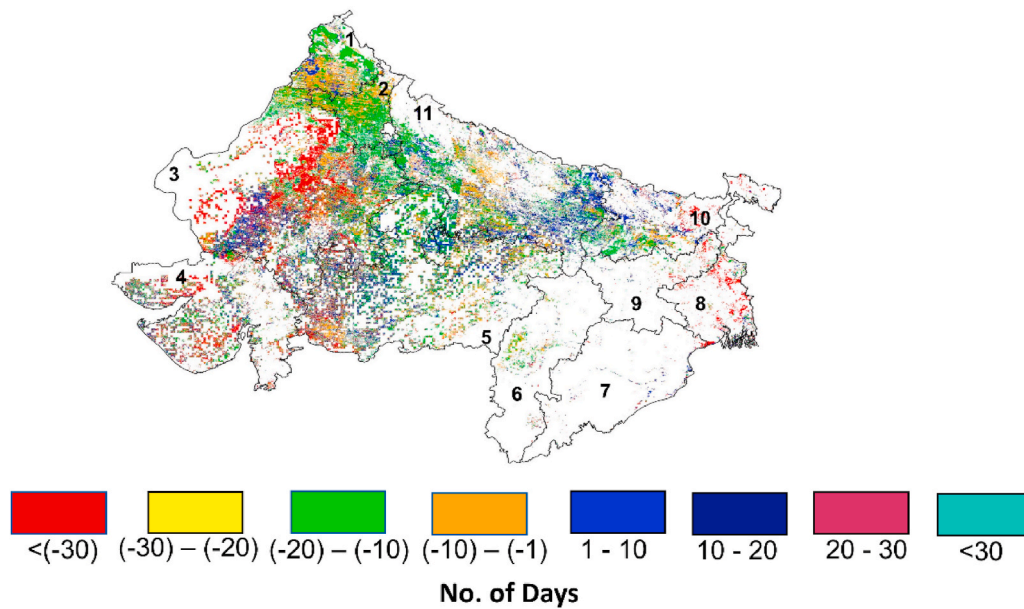
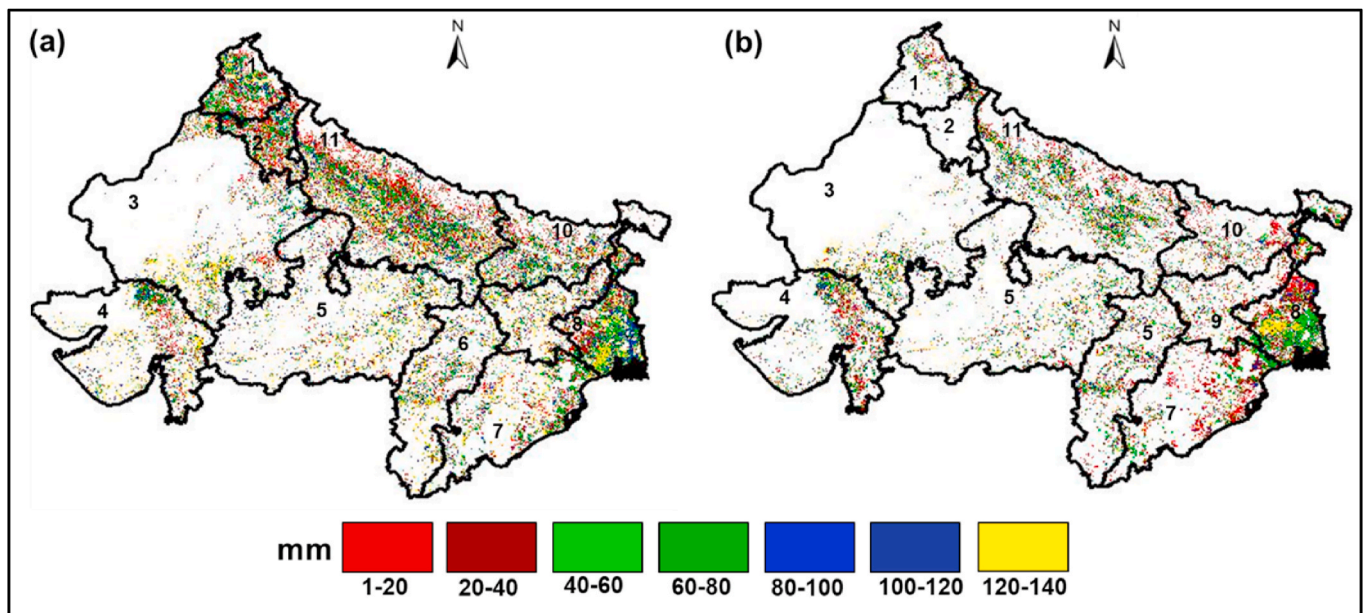


Fig. 8. Spatial distribution of difference of mean and year 2020 harvest date for *rabi* crops.



1. Punjab 2. Haryana 3. Rajasthan 4. Gujarat 5. Madhya Pradesh 6. Chhattisgarh
7. Odisha 8. West Bengal 9. Jharkhand 10. Bihar 11. Uttar Pradesh

Fig. 9. Spatial distribution of deviation in agricultural water demand in with 2020 from mean of 2018 and 2019 during (a) 1–30 April and (b) 1–20 May

maturity and early vegetative stages, respectively in West Bengal state. A less reduction in AWD of 4–5% was observed during April–May which could be due to low radiation, temperature and vapor pressure deficit associated with clouds from norwesters and cyclone of ‘Amphan’ in the second week of May.

In-situ AWD (in mm depth of water) was estimated from the measured pan evaporation data following FAO56 manual (Allen et al., 1998) by applying pan evaporation coefficient (K_p) and crop coefficient (K_c) for respective crops. The mean in-situ AWD was computed for periods 1–30 April and 1–20 May using the data from 2018, 2019 and year 2020. In all the four locations, AWD was found to decrease in 2020 as compared to mean from last two years. The in-situ data showed reductions of 11–59 mm in April and 14–47 mm in May in 2020 at four

agro-meteorological stations.

5. Discussion

With India under lockdown, the country’s electricity consumption has fallen by nearly 19% as recorded in the first week of April 2020 as compared to pre-lockdown phase. Coal-based power generation was reduced by 26% in the two weeks after the lockdown was announced as compared to two weeks before. The consumption of petroleum products in India was decreased by 18%. Anthropogenic emissions through biomass burning, fossil fuel consumption and coal-based power plant emissions are the major sources of NO_2 . Moreover, the NO_2 emissions are always coupled with heat release. There is a reduction of

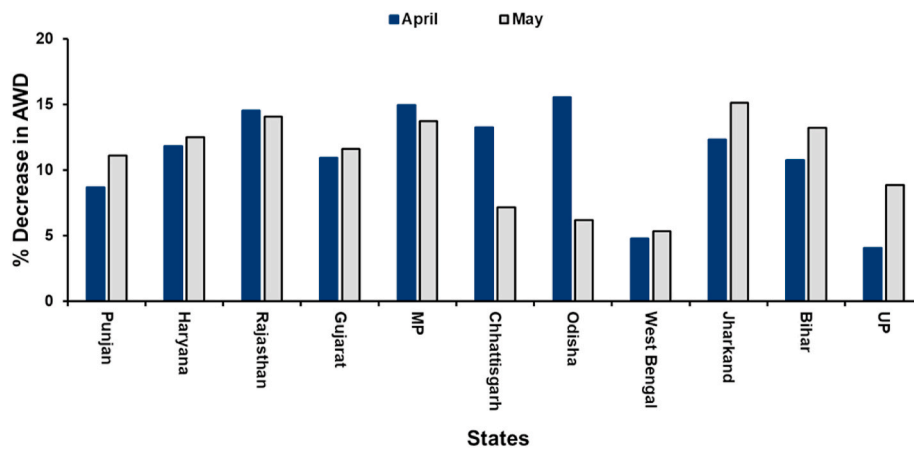


Fig. 10. Percent decrease in AWD in year 2020 as compared to mean of two previous years' in selected states of India.

atmospheric NO₂ concentration in the range up to 18% in the first 21 days of lockdown (Pathakoti et al., 2020). It is quite obvious that there was a substantial reduction in the heat release as also evidenced through reduced power consumption. Though NO₂ is not a green-house-gas (GHG) its spatio-temporal variability influences ozone cycle and surface ozone concentration which acts as GHG (Ghorai et al., 2015). Therefore, likely reduction of surface ozone coupled with large-scale substantial reduction in NO₂ might have also contributed to surface cooling. Temporary reductions in daily atmospheric CO₂, an important GHG, was also reported at global scale during forced lockdown due to COVID-19 (Quere et al., 2020). All these are possible factors for surface cooling. In contrary, it may be noted that there was an increase in incident light energy of the order of 10–30% (Bhattacharya and Desai, 2020) over Indian sub-continent with a range of 10–50% which suggests increased incident photosynthetically active radiation (IPAR) in 0.4–0.7 μm and surface insolation in the shortwave range (0.3–3 μm) during daytime due to strong reduction in Aerosol Optical Depth (AOD) to the maximum of 25% over majority of the Indian region during nationwide lockdown (Pathakoti et al., 2020). The increased surface insolation might cause relative increase in daytime surface heating which generally follows an exponential decay since evening to midnight. The trade-off between thermal cooling and residual impact of increased daytime insolation on nighttime heating ultimately led to overall nighttime surface cooling. It is difficult to decouple effect of shortwave radiation and ground heat load sources on thermal emission during daytime which is beyond the scope this paper. In addition to above factors, analysis of surface soil moisture data in major industrial clusters also showed decrease mean soil moisture across March and April 2020, indicating no major rainfall event during the study period. Bhilai steel plant in the state of Chhattisgarh showed highest reduction (6%) in soil moisture within these two months.

With reference to reduced vegetation fires, it is likely to be argued that the reduction in number of forest fires can also be due to possible rains during this period. Intermittent rains during summer season, tend to build soil moisture and thus reduce forest fires. Fires are unlikely to occur if the forest floor is wet (or having moisture). It is, therefore, pertinent to identify the root cause, whether reduction in vegetation fires is because of rains or as a result of reduced movement of people. To investigate possibility of rains, monthly mean soil moisture from NASA-SMAP data was analyzed for month of March and April (Fig. 11) that showed declined soil moisture trend in these two months, which suggest that no significant moisture built-up due to rainfall occurred in this period. Lower soil moisture levels in April 2020 than the previous month were noticed, indicating normal and natural drying trend in soil moisture with progress of summer in all the states, except Karnataka and Kerala; indicating reduced number of vegetation fires is a result of reduced anthropogenic activities rather than natural factors. This clearly

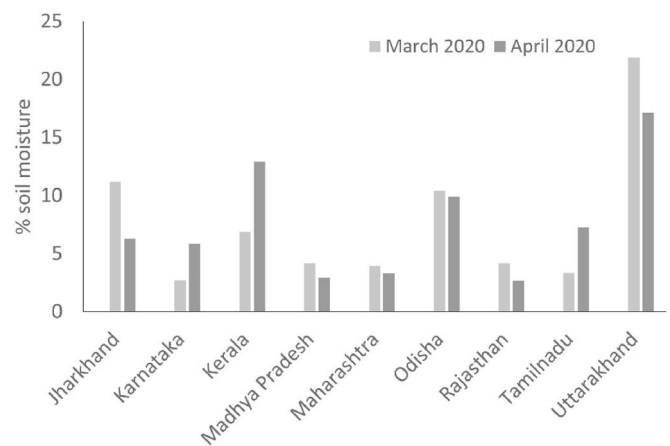


Fig. 11. Soil moisture variations in March and April 2020 indicating normal and natural drying trend in soil moisture in majority of the states.

eliminates 'rain' as possible cause of reduced fires and strengthens that movements of people during lockdown were severely restricted, thereby reducing vegetation fire occurrences.

The multi-year analysis for harvest date clearly indicated a substantial delay in harvesting dates of *rabi* crops in northern, north-western, central and parts of eastern India. In India, harvesting depends on availability of workers after crop maturity. The temporary restrictions imposed during initial phase of lockdown due to COVID-19 made the harvest operations little delayed which could be detected by multi-temporal satellite data and developed model. The validation of the model also resulted into high R² with RMSE of the order of 4 days. This indicated that a net delay of 1–2 weeks in *rabi* harvest could be due to temporary lockdown. It is imperative to know whether this delay coupled with better quality of environment during lockdown had any positive or negative impact on *rabi* agricultural productivity. Further analysis with MODIS GPP product over agricultural area showed consistent increase in *rabi* agricultural productivity to the tune 20–32% (Fig. 12). It proved that delay in *rabi* harvest due to temporary restrictions in lockdown had practically no impact on agricultural productivity rather facilitated in having better harvest which could be due to better environmental quality from reduced particulate matter or aerosol loading over Indian region (Pathakoti et al., 2020) allowing higher light energy (Bhattacharya and Desai, 2020) maximum up to 50% for photosynthesis in daytime and lesser respiration due to large-area night-time cooling (section 4.1) during lockdown to result into higher net carbon uptake.

As explained in previous section, substantial reduction in AWD was

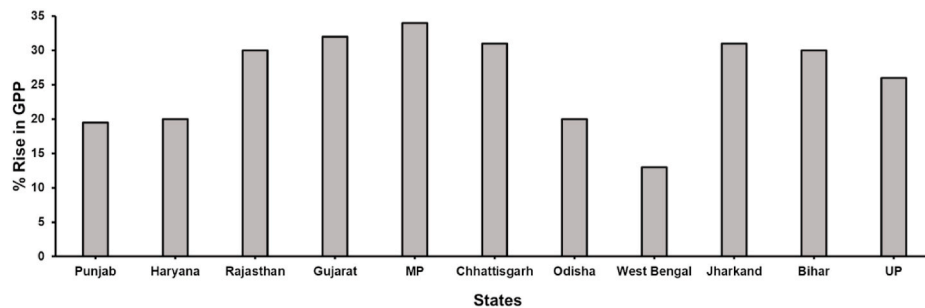


Fig. 12. Change in *rabi* agricultural productivity in 2020 as compared to mean from previous four years.

noticed in Centre and Central-Western states of the country. It may be noted that during the year 2020, no significant loss in agriculture was reported during January to May in northern and north-western parts of India due to any natural disasters such as hailstorm, unseasonal rainfall etc. Therefore, the reduced AWD was clearly due to environmental impact of lockdown especially over northern, north-west, central India and parts of eastern India which did not witness significant impact due to natural disasters. The environmental impact of lockdown on AWD was verified by comparing reduction in satellite-derived AWD with decrease in pan evaporation data in April and May at selected agrometeorological station locations of north and north-west India. The reduction in satellite estimated AWD matches well with reductions in-situ AWD (Fig. 13). The comparison of in-situ and satellite-based estimates showed a deviation of 18.8% from observed mean.

The interaction of solar insolation and land surface govern the meteorological variables such as wind speed, air temperature, humidity and vapor pressure deficit and govern the land surface fluxes (Bastiaanssen 1998; Zhang et al. 2012, 2016). These fluxes are responsible for energy and mass exchange in soil-atmosphere continuum (Betts et al., 1996). The evapotranspiration is a process which govern both energy and mass exchange. The reduction in mean daily temperatures due to cooling in night-time temperature leads to reduction in daily vapor pressure deficit, that further leads to reduction in reference evapotranspiration (Vyas et al., 2016). As losses in transpiration are reduced, there is a reduction in the demand of water for agriculture use (Allen et al., 1998; Allen, 1999).

6. Conclusion

The present study has been carried out to assess the effect of 'lockdown' or restricted human activities due to the COVID-19 pandemic in India on several new aspects by analyzing satellite-based novel parameters which were not reported earlier. Overall, it brought out some positive spin-offs due to lockdown which can be taken into account for making future strategy on sustainable environment for achieving related Sustainable Development Goals (SDGs). The major conclusions from the above study are following:

- Substantial night-time surface cooling of the order of 2–6 K was evident due to lockdown over several cities having continental climate and patches of large industrial congregations when there was no intermittent build-up of surface soil moisture. This is primarily attributed to temporary reduction of heat sources from combustion and partly due to reduction in GHG and pollutant gases.
- A substantial reduction in vegetation fire counts in the order of 5–75% was noticed from space-based data in majority of Indian states during fire-prone period, March–April, of 2020 as compared to mean from previous years'. Increase in primary productivity to the tune of maximum 38% was noticed over Indian forests.
- Though a delay in *rabi* crop harvest for 1–2 weeks was noticed the overall agricultural productivity increased in north Indian states to a maximum of 34% which is attributed to favorable environmental

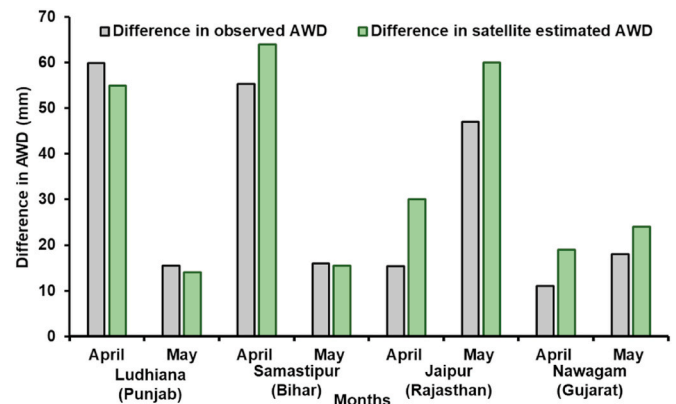


Fig. 13. Comparison of AWD difference between mean (from 2018, 2019) and 2020 from in situ and satellite-based estimates at selected agrometeorological stations of north and north-west India.

conditions and increased net carbon assimilation owing to delayed harvest.

- Agricultural water demand was found to show substantial reduction to the tune of 5–15% in majority of north Indian states. This can also help in meeting less water requirements either through irrigation or rainfall. In a way, it might have led to a substantial water saving for agriculture.

These provide evidence of improvements in various metrics within peri-urban, urban, agriculture and forest ecosystems which are possible if the anthropogenic pressure can be rationally handled for better environment and subsequent impact on ecosystems in terms of better human comfort, low carbon footprint and emissions, reduced forest loss, higher agricultural productivity and water saving.

Ethical statement

All ethical practices have been followed in relation to the development, writing and publication of the article.

CRediT authorship contribution statement

Nikhil Lele: Investigation, Data curation, Formal analysis, Writing - original draft. **Rahul Nigam:** Data curation, Formal analysis, Writing - original draft. **Bimal K. Bhattacharya:** Conceptualization, Data curation, Writing - review & editing, Supervision.

Declaration of competing interest

The authors declare that they have no known conflict of financial interests or personal relationships that could have appeared to influence the work reported in this paper.

References

- OpenStreetMap. Accessed in June 2020. www.openstreetmap.org. Accessed on. www.covid19.who.int-. (Accessed 5 August 2020).
- Accessed on. www.earthdata.nasa.gov-. (Accessed 1 August 2020).
- Accessed on. www.mosdac.gov.in-. (Accessed 19 August 2020).
- Accessed on. www.worldometers.info/world-population/India-population. (Accessed 10 October 2020).
- Alam, Mohammad, 2016. Shifting Cultivation in North-East India: Trends, Benefits and Challenges.
- Allen, R., 1999. Regional Advection Perturbations in an Irrigated Desert (RAPID) - Impacts on Evapotranspiration. University of Idaho/Wageningen Agricultural University/Utah State University. Initial Report, 12. <http://www.kimberly.uidaho.edu/~rallen/equip/rapidrp1.pdf>.
- Allen, R.G., Pereira, L.S., Raes, D., Smith, M., 1998. Crop Evapotranspiration: Guidelines for Computing Crop Water Requirements. In: FAO Irrigation and Drainage PaperNo, vol. 56. FAO, Rome.
- Anonymous, 2019. Package of practices for crops of Punjab rabi, 36 (2), 2278–3709. ISSN.
- Bastiaansen, W.G.M., Menenti, M., Feddes, R.A., Holtslag, A.A.M., 1998. A remote sensing surface energy balance algorithm for land (SEBAL). 1. Formulation. *J. Hydrol.* 212–213, 198–212. [https://doi.org/10.1016/S0022-1694\(98\)00253-4](https://doi.org/10.1016/S0022-1694(98)00253-4).
- Bermen, J.D., Keita, E., 2020. Changes in U.S. air pollution during the COVID-19 pandemic. *Sci. Total Environ.* 739 <https://doi.org/10.1016/j.scitotenv.2020.139864>, 139864.
- Betts, Alan K., Ball, John H., Anton, C., Beljaars, M., Miller, Martin J., Viterbo, Pedro A., 1996. The land surface-atmosphere interaction: a review based on observational and global modelling perspectives. *J. Geophys. Res.: Atmospheres* 101 (D3), 7209–7225. <https://doi.org/10.1029/95jd02135>.
- Bhattacharya, S.B., Desai, D., 2020. Change Detection of Incident Light over Indian Sub-continent during Covid-19 Lockdown Using Satellite Imaging Data. in: Proceedings of IEEE International India Geoscience and Remote Sensing Symposium (InGARSS) 2020, pp. 162–165, 978-1-7281-3114-6. <https://www.ingarss200.org/dashboard.php>.
- Choudhury, I., Bhattacharya, B.K., 2018. An assessment of satellite-based agricultural water productivity over the Indian region. *Int. J. Rem. Sens.* 39, 2294–2311.
- Das, M., Arijit, Das, Raju, Sarkar, Sunil, Saha, Ashis, Mandal, 2020. Examining the impact of lockdown (due to COVID-19) on ambient aerosols (PM_{2.5}): a study on indo-gangetic plain (IGP) cities, India stochastic environmental research and risk assessment. <https://doi.org/10.1007/s00477-020-01905-x>(0123).
- Das, M., Arijit, Das, Sasanka, Ghosh, Raju, Sarkar, Sunil, Saha, 2021. Spatio-temporal concentration of atmospheric particulate matter (PM_{2.5}) during pandemic: a study on most polluted cities of indo-gangetic plain. *Urban Climate* (2021) 100758. <https://doi.org/10.1007/s00477-020-01905-x>(0123, 35).
- Fsi, 2015. State of Forest Report Year 2015. Forest Survey of India, Dehradun (India).
- Gao, F., Schaaf, C.B., Strahler, A.H., Roess, A., Lucht, W., Dickinson, R., 2005. MODIS bidirectional reflectance function and albedo climate modeling grid products and variability for albedo for major global vegetation types. *J. Geophys. Res.* 110 (D1104).
- Garg, Vaibhav, Prasad Aggarwal, Shiv, Chauhan, Prakash, 2020. Changes in turbidity along Ganga River using Sentinel-2 satellite data during lockdown associated with COVID-19. *Geomatics, Nat. Hazards Risk* 11 (1), 1175–1195. <https://doi.org/10.1080/19475705.2020.1782482>.
- Giglio, L., Wilfrid Schroeder, Christopher O. Justice, 2016. The Collection 6 MODIS Active fire algorithm. *Rem. Sens. Environ.* 178, 31–41.
- Gorai, A.K., Tuluri, F., Tchounwou, P.B., Ambinakudige, S., 2015. Influence of local meteorology and NO₂ conditions on ground-level ozone concentrations in the eastern part of Texas, USA. *Air Qual. Atmos. Health* 8, 81–96. <https://doi.org/10.1007/s11869-014-0276-5>.
- Gupta, Amitesh, Bhatt, C.M., Roy, Arijit, Chauhan, Prakash, 2020. COVID 19 lockdown a window of opportunity to understand role of human activity on forest fire incidences in the Western Himalaya, India. *Curr. Sci.* 119 (2), 390–398.
- Holmes, T.R.H., Crow, W.T., Hain, C., 2013. Spatial pattern in timing of diurnal temperature cycle. *Hydrol. Earth Syst. Sci.* 17, 3695–3706.
- Huete, A., Didan, K., Leeuwen, W.V., 1999. MODIS Vegetation Index (MOD-13) Algorithm Theoretical Basis Document.
- Imd, 2014. INSAT 3-D Product Catalogue. Indian Meteorological Department, New Delhi.
- Invest India, 2020. Great places for manufacturing in India. www.investindia.gov, 1.
- Jaglan, M.S., Qureshi, M.H., 1996. Irrigation development and its environmental consequences in arid regions of India. *Environ. Manag.* 20, 323–336.
- Jangid, M.K., Sharma, L., Burark, S.S., Jain, H.K., Meena, G.L., 2018. Land use pattern, cropping pattern and resource use efficiency in arid western plain zone of Rajasthan. *Ind. J. Ext. Educ. R.D.* 26.
- Joseph, Shijo, Anitha, K., Murthy, M.S.R., 2009. *J. For. Res.* 14, 127–134.
- Lal, Preet, Amit, Kumar, Kumar, Shubham, Sheetal, Kumari, Purabi, Saikia, Arun, Dayanandan, Adhikari, Dibyendu, Khan, Mohammed, 2020. The dark cloud with a silver lining: assessing the impact of the SARS COVID-19 pandemic on the global environment. *Sci. Total Environ.* 732, 139297.
- Lata, A., 2014. Changing pattern of crops and land use during post reform period in Haryana: a geographical analysis. *Res. J. Human. Soc. Sci.* 2 (9), 15–20.
- Lokhandwala, Snehal, Pratibha, Gautam, 2020. Indirect impact of COVID-19 on environment: a brief study in Indian context. *Environ. Res.* <https://doi.org/10.1016/j.envres.2020.109807>, 109807.
- Mahato, Susanta, Pal, Swades, Ghosh, Krishna Gopal, 2020. Effect of lockdown amid COVID-19 pandemic on the air quality of the megacity, Delhi, India. *Sci. Total Environ.* 730, 139086. In press. <https://doi.org/10.1016/j.scitotenv.2020.139086>.
- Mark, McDonnell, MacGregor-Fors, Ian, 2016. The ecological future of cities. *Science* 352 (6288), 936–938.
- Mathison, C., Deva, C., Falloon, P., Challinor, A.J., 2018. Estimating sowing and harvest dates based on the Asian summer monsoon. *Earth Syst. Dyn.* 9, 563–592.
- Meena, A.L., Bisht, P., 2017. Regional study of variation in cropping and irrigation intensity in Rajasthan state, India. *Sustain. Agri. Food Environ. Res.* 5 (4) <https://doi.org/10.7770/safer-V5N4-art1314>.
- MoAF&W, 2017. Ministry of Agriculture and Farmer Welfare. Govt of India, 2017.
- Monteith, J.L., 1977. Climate and the efficiency of crop production in Britain. *Philos. Trans. R. Soc. Lond. B Biol. Sci.* 281, 277–294.
- Nakada, L.Y.K., Urban, R.C., 2020. COVID-19 pandemic: impacts on the air quality during the partial lockdown in São Paulo state, Brazil. *Sci. Total Environ.* 730, 139087. [https://nfsm.gov.in/National food security mission Govt of India](https://nfsm.gov.in/National%20food%20security%20mission%20Govt%20of%20India). Accessed in July 2020.
- Nigam, R., Bhattacharya, B.K., 2015. Potential Evapotranspiration (PET) from INSAT 3D Insolation Product and Short -range Forecasts. INSAT 3-D Algorithm Theoretical Basis Document.
- Nrsc, 2014. National Resources Census- Land Use Land Cover Database. National Remote sensing Center, Hyderabad, India. Technical Report no. 1.
- Pathakoti, M., Aarathi, M., Hazra, S., Mahalakshmi, D., Raja Shekhar, Srinivasulu J., Sesha Sai, M., Prasad, A., Uma, V., 2020. An Assessment of the impact of a nationwide lockdown on air pollution- a remote sensing perspective over India. *Atmos. Chem. Phys.* <https://doi.org/10.5194/acp-2020-621>.
- Pinki, Lekha, H., Rana, S., 2013. Pattern of crop diversification in Haryana. *Res. J. Human. Soc. Sci.* 4 (3), 405–409.
- Quere Le, C., Jackson, B.R., et al., 2020. Temporary reductions in daily global CO₂ emissions during the COVID-19 forced confinement. *Nat. Clim. Change* 10, 647–653. <https://doi.org/10.1038/s41558-020-0797-x>.
- Running, S.W., Thornton, P.E., Nemani, R.R., Glassy, J.M., 2000. Global Terrestrial Gross and Net Primary Productivity from the Earth Observing System. In: Sala, O., Jackson, R., Mooney, H. (Eds.), *Methods in Ecosystem Science*. Springer-Verlag, New York, pp. 44–57.
- Sakamoto, T., Yokozawa, Masayuki, Toritani, Hitoshi, Shibayama, Michio, Ishitsuka, Naoki, Ohno, Hroyuki, 2005. A crop phenology detection method using time-series MODIS data. *Rem. Sens. Environ.* 96 (3–4), 366–374.
- Satendra, Kaushik, A.D., 2014. Forest Fire Disaster Management. National Institute of Disaster Management, New Delhi India, p. 67. Ministry of Home Affairs. NIDM.
- Selvam, S., Jesuraja, K., Venkatraman, S., Chung, S.Y., Roy, P.D., Muthukumar, P., Kumar, Manish, 2020. Imprints of pandemic lockdown on subsurface water quality in the coastal industrial city of Tuticorin, South India: a revival perspective. *Sci. Total Environ.* 738, 139848.
- Sharma, N., Singh, S.P., 2014. Agricultural diversification in Indian Punjab: an assessment of government intervention through contract farming. *J. Agric. Food Inf.* 15 (3), 191–213.
- Sharma, Shubham, Zhang, Mengyuan, Anshika, Gao, Jingsi, Zhang, Hongliang, Kota, Sri, 2020. Effect of restricted emissions during COVID-19 on air quality in India. *Sci. Total Environ.* 728 <https://doi.org/10.1016/j.scitotenv.2020.138878>, 138878.
- Shehzad, Khurram, Sarfraz, Muddassar, Meran Shah, Syed Ghulam, 2020. The impact of COVID-19 as a necessary evil on air pollution in India during the lockdown. *Environ. Pollut.* 266 <https://doi.org/10.1016/j.envpol.2020.115080>, 115080.
- Shweta, Bimal K., Bhattacharya, Pramod Krishna, Akhouri, 2018. A baseline regional evapotranspiration (ET) and change hotspots over indian sub-tropics using satellite remote sensing data. *Agric. Water Manag.* 208, 284–298.
- Siddiqui, Asfa, Suvankar Halder, Chauhan, Prakash, Kumar, Pramod, 2020. COVID-19 pandemic and city-level nitrogen dioxide (NO₂) reduction for urban centres of India. *J. Indian Soc. Rem. Sens.* 48, 999–1006. <https://doi.org/10.1007/s12524-020-01130-7>.
- Singh, R.P., Chauhan, A., 2020. Impact of lockdown on air quality in India during COVID-19 pandemic. *Air Qual. Atmos. Health* 13, 921–928. <https://doi.org/10.1007/s11869-020-00863-1>.
- Somani, M., Srivastava, Abhishek N., Kumar Gummadivalli, Shiva, Sharma, Aparna, 2020. Indirect implications of COVID-19 towards sustainable environment: an investigation in Indian context. *Bioresour. Technol. Rep.* 11 <https://doi.org/10.1016/j.biteb.2020.100491>, 100491.
- Srivastava, Sudhakar, Amit, Kumar, Baudhdh, Kuldeep, Sagar Gautam, Alok, Kumar, Sanjeev, 2020. 21-Day lockdown in India dramatically reduced air pollution indices in Lucknow and New Delhi, India. *Bull. Environ. Contam. Toxicol.* 105, 9–17. <https://doi.org/10.1007/s00128-020-02895-w>.
- Vyas, Swapnil, Nigam, Rahul, Patel, N.K., Panigrahy, Sushma, 2013. Extracting regional pattern of Wheat sowing dates using multispectral and high temporal observations from Indian Geostationary satellite. *J. Indian Soc. Rem. Sens.* 41, 855–864.
- Vyas, S., Nigam, R., Bhattacharya, B.K., Kumar, P., 2016. Development of real-time reference evapotranspiration at the regional scale using satellite-based observations. *Int. J. Rem. Sens.* 37, 6108–6126.
- Wan, 1999. MODIS Land-Surface Temperature Algorithm Theoretical Basis Document (LST ATBD). Institute for computation Earth System Science, Santa Barbara.
- Yunus, A.P., Yoshifumi Masago, b, Hijioaka, Yasuaki, 2020. COVID-19 and surface water quality: improved lake water quality during the lockdown. *Sci. Total Environ.* 731, 139012.

Zambrano-Monserrate, M.A., Ruano, M.A., Sanchez-Alcalde, L., 2020. Indirect effects of COVID-19 on the environment. *Sci. Total Environ.* 728 <https://doi.org/10.1016/j.scitotenv.2020.138813>, 138813.

Zhang, Yongqiang, Ray, Leuning, Chiew, Francis H.S., Wang, Enli, Zhang, Lu, Liu, Changming, Sun, Fubao, Peel, Murray C., Shen, Yanjun, Jung, Martin, 2012.

Decadal trends in evaporation from global energy and water balances. *J. Hydrometeorol.* 13 (1), 379–391. <https://doi.org/10.1175/jhm-d>.

Zhang, Yongqiang, Peña-Arancibia, Jorge L., McVicar, Tim R., Chiew, Francis H.S., Vaze, Jai, Liu, Changming, Lu, Xingjie, et al., 2016. Multi-decadal trends in global terrestrial evapotranspiration and its components. *Sci. Rep.* 6 (1) <https://doi.org/10.1038/srep19124>.